Feature Weighted Active Contours for Image Segmentation

Bing Li and Scott T. Acton
Charles L. Brown Department of Electrical and Computer Engineering
University of Virginia, Charlottesville, VA 22904 USA
E-mail: {bingli, acton}@virginia.edu

Abstract

A novel external energy construction for active contours is proposed in this paper. In contrast to the standard approach of using linear filtering to smooth the external energies and to avoid noise, we define feature weighted active contours for extracting features of interest without distortion. The advantages of this innovation are demonstrated by examples and comparisons with Gaussian filtered external energy. Compared to the linear filtering approach, the feature weighted active contours yield lower root mean squared errors of contour position and improve upon the ability to capture fine details in noisy images.

1. Introduction

Snakes [1], or *active contours*, have been widely used for image segmentation [2-4] and tracking [5-7]. Snakes are curves that can deform within the image plane and capture a desired feature. The snake evolution method is modeled as minimizing an energy functional subject to certain constraints. The energy functional usually contains two terms: an internal energy, which constrains the smoothness and tautness of the contour, and an external energy, which attracts the contour to the features of interest.

Typical external energy formulations employ a Gaussian filter or another appropriate filter to mitigate the sensitivity to image noise; however, the filtering also distorts the features of interest. In this case, the standard deviation of the Gaussian filter governs the tradeoff between the preservation of desired features and the suppression of the noise. As a result, fine features are very difficult to capture for active contours in a noisy image. In this paper, we propose a novel external energy to address this problem by designing a weighting function. We focus on parametric active contours in this paper, though the result could be easily generalized to geometric active contours [8] and to higher dimensionality [9]. A comparison of results using different external forces on noisy images is presented that reveals the efficacy of our method.

2. Background

An active contour is represented by a parametric curve $\mathbf{x}(s) = [x(s), y(s)]$, $s \in [0,1]$, that deforms through the image domain to minimize the energy functional

$$E_{AC} = \int_0^1 \left[\frac{1}{2}\left(\alpha \left|\mathbf{x}'(s)\right|^2 + \beta \left|\mathbf{x}''(s)\right|^2 \right) + E_{\text{ext}}\left(\mathbf{x}(s)\right) \right] ds \quad (1)$$

where α and β are weighting parameters representing the degree of the smoothness and tautness of the contour, respectively, and $\mathbf{x}'(s)$ and $\mathbf{x}''(s)$ are the first and second derivatives of $\mathbf{x}(s)$ with respect to *s*. E_{ext} denotes the external energy, the value of which is small at the features of interest. Typical external energies for a gray-level image $I(x,y)$ for seeking the edges are given as [1]

$$E_{\text{ext}}^{(1)}(x,y) = -\left|\nabla I(x,y)\right|^2, \quad (2)$$

$$E_{\text{ext}}^{(2)}(x,y) = -\left|\nabla\left[G_\sigma(x,y) * I(x,y)\right]\right|^2 \quad (3)$$

where $G_\sigma(x,y)$ is a 2D Gaussian function with standard deviation σ, $*$ denotes linear convolution, and ∇ denotes the gradient operator . If the image is binary image, where the features of interest are one and the background is zero, the typical external energies are given as [10]

$$E_{\text{ext}}^{(3)}(x,y) = -I(x,y), \quad (4)$$

$$E_{\text{ext}}^{(4)}(x,y) = -G_\sigma(x,y) * I(x,y). \quad (5)$$

To minimize (1), the contour must satisfy the Euler equation

$$\alpha \mathbf{x}''(s) - \beta \mathbf{x}''''(s) - \nabla E_{\text{ext}} = 0, \quad (6)$$

which can be considered as a force balance equation

$$\mathbf{F}_{\text{int}} + \mathbf{F}_{ext} = 0 \quad (7)$$

where $\mathbf{F}_{\text{int}} = \alpha \mathbf{x}''(s) - \beta \mathbf{x}''''(s)$ is the internal force to constraint the contour smoothness and $\mathbf{F}_{ext} = -\nabla E_{\text{ext}}$ is the external force to attract the contour toward the features of interest.

To solve (6), $\mathbf{x}(s)$ is treated as a function of time *t* as well as of parameter *s*, and the solution is obtained when the steady state solution of the following gradient descent equation is reached from an initial contour $\mathbf{x}(s,0)$

$$\frac{\partial \mathbf{x}(s,t)}{\partial t} = \alpha \mathbf{x}''(s,t) - \beta \mathbf{x}''''(s,t) + \mathbf{F}_{ext}. \quad (8)$$

A solution to (8) on a discrete grid can be achieved by solving the discretized equation iteratively using a finite difference approach [1].

The *gradient vector flow* (GVF) field is the vector field $\mathbf{v}(x,y) = [u(x,y), v(x,y)]$ that minimizes the energy functional

$$E_{GVF} = \iint \left[\mu \left(|\nabla u|^2 + |\nabla v|^2 \right) + |\nabla f|^2 |\mathbf{v} - \nabla f|^2 \right] dxdy \quad (9)$$

where $f = -E_{\text{ext}}$ is an *edge map* derived from the image, and μ is a fundamental parameter controlling the degree of smoothness of the vector field. As shown in [11], the GVF field has a large capture range and the ability to progress into concavities. By replacing the external force $\mathbf{F}_{ext}$ in (8) by the GVF field $\mathbf{v}$, the solution for GVF active contours can be written as

$$\frac{\partial \mathbf{x}(s,t)}{\partial t} = \alpha \mathbf{x}''(s,t) - \beta \mathbf{x}''''(s,t) + \mathbf{v}. \quad (10)$$

3. Feature Weighted Active Contours

We propose the *feature weighted* (FW) active contour external energy functional

$$E_{\text{ext}}^{FW}(x,y) = w(S(x,y)) E_{\text{ext}}^{(p)}(x,y) \quad (11)$$

where $E_{\text{ext}}^{(p)}(x,y)$ is the standard external force, which is usually unfiltered or Gaussian filtered with a small standard deviation σ, $w(S(x,y))$ is the *weighting function* of the *feature score* $S(x,y)$ at (x,y). The feature score is employed to distinguish desired features from others. The weighting function is designed to be close to one at desired features and close to zero otherwise. Note that $E_{\text{ext}}^{(p)}(x,y)$ is less than or equal to zero, the FW active contours will not be distracted by undesired features with low external energy, such as noise and clutters, because the external energy of undesired features is scaled to nearly zero. The FW external energy can be viewed as a non-linear filtered version of the standard external energy. Two weighting functions are proposed in the following sections for distinct applications.

3.1. Area Based Weighting

Based on the observation that the noise is manifested as a collection of impulses and edges of objects are contiguous 2D contours, the *area based* (AB) weighting function is given as

$$w_{AB}(S_{AB}(x,y)) = 1 - \exp\left\{ -S_{AB}(x,y)^2 / a^2 \right\} \quad (12)$$

where *a* is a soft threshold, which should be increased with increased noise variance. The feature score $S_{AB}(x,y)$ can be calculated by counting the number of pixels (*i.e.*, the area) of the connected *strong features* at (x,y). A strong feature is present if the standard external energy $E_{\text{ext}}^{(p)}$ at (x,y) is less than a certain threshold τ, which is determined by the minimum edge length to be preserved. We set the threshold to $\tau = -2\sqrt{\mu}$ in our application, where μ is the GVF weighting parameter in (9). We also note that if

$$w'_{AB}(S_{AB}(x,y)) = \begin{cases} 1, S_{AB}(x,y) \geq a \\ 0, S_{AB}(x,y) < a \end{cases}, \quad (13)$$

then this process is equivalent to an area open morphological filter. Although both weight functions are valid, (12) leads to a soft threshold where (13) yields a hard threshold. Morphological filters could be employed to connect the strong features if the image is noisy and strong features are not contiguous.

Note that the AB weighting function w_{AB} is close to one if the area of the connected strong features is much larger than *a*, and close to zero if the area is small.

3.2. Cross-Correlation Based Weighting

In a noisy image, the desired edges may be broken or weak, and the snake could be "distracted" by nearby strong edges. By considering the prior shape information, clutter can be eradicated. An edge template T is defined by a set of coordinates $\{(m_i, n_i); i = 1, ..., M\}$, which is centered around $(0,0)$. Let $T^\dagger$ denote the mirrored edge template defined by a set of coordinates $\{(-m_i, -n_i); i = 1, \ldots, M\}$ and $T \Diamond I(x, y)$ denote the set of image I pixels covered by the edge template T centered at (x, y). A pixel p in image I *participates* in the cross-correlation $\sum T \Diamond I(x, y)$ if $p \in T \Diamond I(x, y)$. The *cross-correlation based* (CCB) weighting function is given as

$$w_{CCB}(S_{CCB}(x, y)) = \begin{cases} 0 & , S_{CCB}(x, y) < c \\ \dfrac{S_{CCB}(x, y) - c}{n} & , otherwsie \end{cases} \quad (14)$$

where $n = \max_{x,y} S_{CCB}(x, y) - c$ is a normalization constant, and c is the minimum desired feature score. The feature score $S_{CCB}(x, y)$ is the maximum normalized cross-correlation in which the pixel $-E_{\text{ext}}^{(p)}(x, y)$ participates, given by

$$S_{CCB}(x, y) = \max\left\{T^{\dagger} \Diamond \left(\frac{1}{M} \sum T \Diamond \left[-E_{\text{ext}}^{(p)}(x, y)\right]\right)\right\} \quad (15)$$

which can be implemented as

$$S_{CCB} = \frac{1}{M}\left(-E_{\text{ext}}^{(p)} \otimes T\right) \circ T^{\dagger} = \frac{1}{M}\left(-E_{\text{ext}}^{(p)} * T^{\dagger}\right) \circ T^{\dagger} \quad (16)$$

where $\otimes$ denotes cross-correlation operation and $\circ$ denotes morphological dilation filter.

If an edge matches the edge template T, the feature scores S_{CCB} at all the pixels on the edge will have a high value. In this case, the CCB weighting function w_{CCB} is close to one at all the pixels on the edge; otherwise, the CCB weighting function is close to zero.

A bank of templates can be used together if the shapes are difficult to be characterized as one shape. The final CCB weighting function combines all the CCB weighting functions for all templates.

4. Results

We first compare the snake results using the area based feature weighted (AB-FW) external energy with those using the Gaussian filtered (GF) external energy on a simulated binary image and a magnetic resonance image of the human ankle cartilage. As shown in Fig. 1(a), two independent snakes are initialized in a noise corrupted binary image, where two U-shapes are close to each other. As we can see from Fig. 1(b), the GF external energy with a small σ value fails to overcome the noise, while the GF external energy with a large σ value distorts the edges, as shown in Fig. 1(c). The standard deviation of the Gaussian filter controls the tradeoff between the feature preservation and noise suppression. In contrast, the AB-FW snakes capture the correct boundaries, as shown in Fig. 1(d). To quantify the accuracy of the results using different external energies, the root mean square error (RMSE) is calculated for outer snake and inner snake (denoted by superscripts 1 and 2, respectively). The error of a point on the snake is defined by the minimum distance between the point and the corresponding boundary in the noise-free image. These results reveal the superior performance afforded by the AB-FW external energy.

In Fig. 2(a), two snakes are initialized to capture the inner and outer boundaries of the bright object. The standard deviation of Gaussian filter is chosen to be the minimum integer required for outer snake to overcome the noise. The AB weighting function highlights the features of interest and removes noise and clutter, as shown in Fig. 2(f). As shown in Fig. 2(g), the corners on the bottom and inside the object are blurred by the Gaussian filter, which causes the inner snake failure; while the corners are segmented correctly using the AB-FW external force.

An image containing leukocytes observed *in vivo* is used to evaluate the performance of the snake using the cross-correlation based feature weighed (CCB-FW) external energy, shown in Fig. 3. In this image, two leukocytes roll along the endothelial wall. The endothelial wall yields strong edges, shown in Fig. 3(d), which distract the snakes targeted at the leukocytes. As shown in Fig. 3(h), the CCB weighting function eliminates majority of the edges generated from the wall. The snakes using GF external energy fail because of the broken and weak leukocyte edges, which are captured properly by the CCB-FW snakes.

5. Conclusion

This paper has proposed a new external energy functional for active contours, which has the ability to capture the weak or broken edges and the ability to filter the noise without blurring the features of interest. The external energy is scaled by multiplying the weighting function, which highlights the desired features. The area based weighting function and the cross-correlation based weighting function have been introduced for tailored applications. We showed that the FW active contours are robust to noise and clutter and are able to capture the fine features within noisy medical images. Different weighting functions can be designed for other applications. This novel external energy paradigm can be easily extended to an active surface model for 3D data.

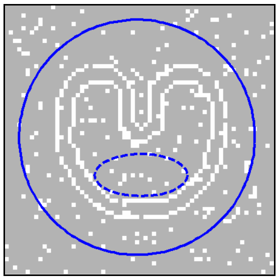

(a)

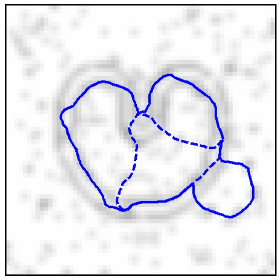

(b) $\text{RMSE}^1 = 4.08$

$\text{RMSE}^2 = 2.74$

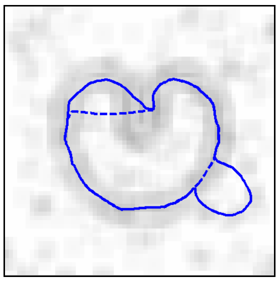

(c) $\text{RMSE}^1 = 3.77$

$\text{RMSE}^2 = 1.88$

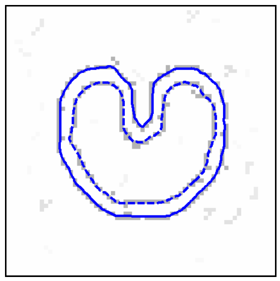

(d) $\text{RMSE}^1 = 0.50$

$\text{RMSE}^2 = 0.48$

Fig. 1. (a) Impulse noise corrupted image and two independent initial snakes; (b) and (c) the GF external energy and snake results using (5) where $\sigma = 1$ and $\sigma = 3$, respectively; (d) the AB-FW external energy and snake results using (12) and (4) where $a = 7$. All results are computed using GVF with $\alpha = 0.3$, $\beta = 0$ and $\mu = 0.1$.

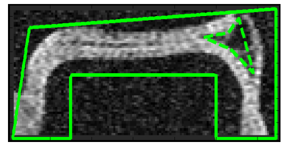

(a)

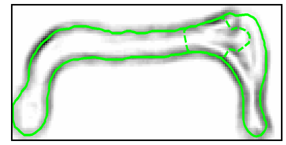

(b)

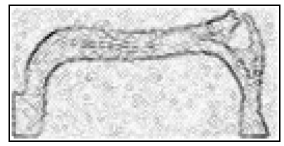

(c)

(d)

(e)

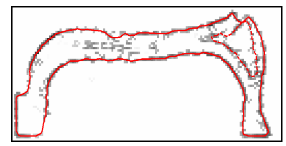

(f)

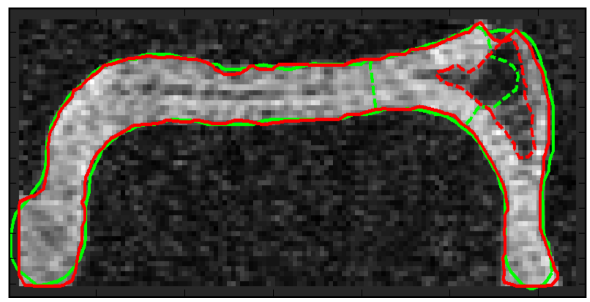

(g)

Fig. 2. (a) A magnetic resonance image of the human ankle cartilage and two independent initial snakes; (b) the GF external energy and snake results using (3) where $\sigma = 4$; (c) the external energy $E_{\text{ext}}^{(p)}$ using (2); (d) the strong features (white); (e) the AB weighting function w_{AB}; (f) the AB-FW external energy and snake results using (12) where $a = 8$; (g) the image superposed with snake results using the GF external energy (green) and the AB-FW external energy (red). All results are computed using GVF with $\alpha = 0.1$, $\beta = 0$ and $\mu = 0.01$.

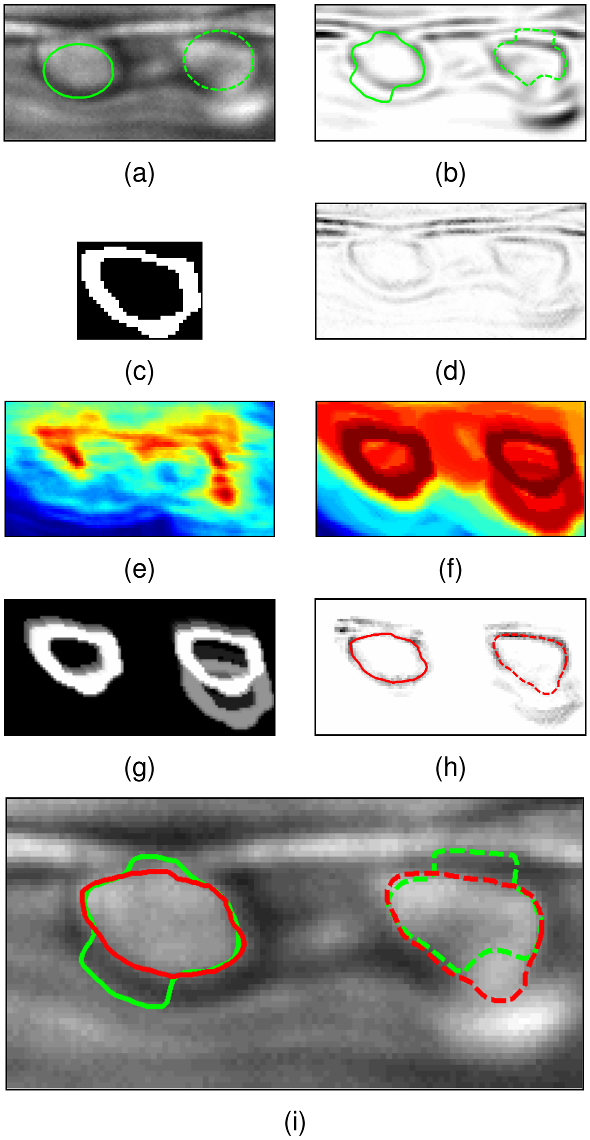

Fig. 3. (a) An image containing leukocytes *in vivo* and two independent initial snakes; (b) the GF external energy and snake results using (3) where $\sigma = 2$; (c) the edge template used for the CCB weighting function; (d) the external energy $E_{\text{ext}}^{(p)}$ using (2); (e) the cross-correlation result and (f) the CCB feature score S_{CCB} (red and blue represent high and low values, respectively); (g) the CCB weighting function w_{CCB}; (h) the CCB-FW external energy and snake results using (14); (i) the image superposed with snake results using the GF external energy (green) and the CCB-FW external energy (red). All results are computed using GVF with $\alpha = 0.25$, $\beta = 0$ and $\mu = 0.01$.

6. References

[1] M. Kass, A. Witkin, and D. Terzopoulos, "Snakes - active contour models," *International Journal of Computer Vision*, vol. 1, pp. 321-331, 1987.

[2] G. Dong, N. Ray, and S. T. Acton, "Intravital leukocyte detection using the gradient inverse coefficient of variation," *Medical Imaging, IEEE Transactions on*, vol. 24, pp. 910-924, 2005.

[3] M. Gastaud, M. Barlaud, and G. Aubert, "Combining shape prior and statistical features for active contour segmentation," *Circuits and Systems for Video Technology, IEEE Transactions on*, vol. 14, pp. 726-734, 2004.

[4] T. F. Chan and L. A. Vese, "Active contours without edges," *Image Processing, IEEE Transactions on*, vol. 10, pp. 266-277, 2001.

[5] N. Ray and S. T. Acton, "Motion gradient vector flow: an external force for tracking rolling leukocytes with shape and size constrained active contours," *Medical Imaging, IEEE Transactions on*, vol. 23, pp. 1466-1478, 2004.

[6] N. Ray, S. T. Acton, and K. Ley, "Tracking leukocytes in vivo with shape and size constrained active contours," *Medical Imaging, IEEE Transactions on*, vol. 21, pp. 1222-1235, 2002.

[7] N. Paragios and R. Deriche, "Geodesic active contours and level sets for the detection and tracking of moving objects," *Pattern Analysis and Machine Intelligence, IEEE Transactions on*, vol. 22, pp. 266-280, 2000.

[8] J. A. Sethian, *Level set methods and fast marching methods: evolving interfaces in computational geometry, fluid mechanics, computer vision, and materials science*. Cambridge University Press, 1999.

[9] D. Terzopoulos, A. Witkin, and M. Kass, "Constraints on deformable models - recovering 3D shape and nonrigid motion," *Artificial Intelligence*, vol. 36, pp. 91-123, 1988.

[10] L. D. Cohen and I. Cohen, "Finite-element methods for active contour models and balloons for 2-D and 3-D images," *Pattern Analysis and Machine Intelligence, IEEE Transactions on*, vol. 15, pp. 1131-1147, 1993.

[11] C. Xu and J. L. Prince, "Snakes, shapes, and gradient vector flow," *Image Processing, IEEE Transactions on*, vol. 7, pp. 359-369, 1998.